

See discussions, stats, and author profiles for this publication at: <https://www.researchgate.net/publication/6980218>

Diffusivity of Asphaltene Molecules by Fluorescence Correlation Spectroscopy

ARTICLE *in* THE JOURNAL OF PHYSICAL CHEMISTRY A · AUGUST 2006

Impact Factor: 2.69 · DOI: 10.1021/jp062099n · Source: PubMed

CITATIONS

75

READS

51

4 AUTHORS:



A. Ballard Andrews

Schlumberger Limited

67 PUBLICATIONS 1,273 CITATIONS

SEE PROFILE



Rodrigo E. Guerra

Harvard University

9 PUBLICATIONS 104 CITATIONS

SEE PROFILE



Oliver C Mullins

Schlumberger Limited

244 PUBLICATIONS 5,948 CITATIONS

SEE PROFILE



Pabitra Sen

University of North Carolina at Chapel Hill

118 PUBLICATIONS 6,094 CITATIONS

SEE PROFILE

Diffusivity of Asphaltene Molecules by Fluorescence Correlation Spectroscopy

A. Ballard Andrews,^{*,†} Rodrigo E. Guerra,^{†,‡} Oliver C. Mullins,[†] and Pabitra N. Sen[†]

Schlumberger-Doll Research, 36 Old Quarry Road, Ridgefield, Connecticut 06877, and
Department of Physics, Harvard University, Cambridge, Massachusetts 22100

Received: April 4, 2006; In Final Form: May 12, 2006

Using fluorescence correlation spectroscopy (FCS) we measure the translational diffusion coefficient of asphaltene molecules in toluene at extremely low concentrations (0.03–3.0 mg/L): where aggregation does not occur. We find that the translational diffusion coefficient of asphaltene molecules in toluene is about $0.35 \times 10^{-5} \text{ cm}^2/\text{s}$ at room temperature. This diffusion coefficient corresponds to a hydrodynamic radius of approximately 1 nm. These data confirm previously estimated size from rotational diffusion studied using fluorescence depolarization. The implication of this concurrence is that asphaltene molecular structures are monomeric, not polymeric.

Introduction

Aptly termed the “cholesterol of petroleum”, asphaltenes are the heaviest, most aromatic component of crude oils defined as the fraction of crude oil that is soluble in toluene and insoluble in *n*-heptane. Asphaltenes are complex compounds consisting of aromatic rings and aliphatic side chains, with a carbon–hydrogen ratio of 1:1.2 with 40% of the carbon in aromatic structures and 90% of the hydrogen on saturated carbon. Every stage of petroleum extraction and production is hindered by the presence of asphaltenes. These molecules separate from the lighter oil phase due to changes in temperature, pressure, or composition forming aggregates that cause pipeline blockage and reduced permeability of subsurface formations. They are also known to stabilize oil/water emulsions, form coke upon heating, and deactivate cracking catalysts—critical steps in the refining process.

Understanding of the basic physics of this aggregation is of central importance to the oil industry and is of great scientific interest. Though significant progress has been made in determining both structural and aggregation properties of asphaltenes,^{1–4} there remain controversies surrounding such basic parameters as the size of asphaltene molecules. Values reported in the literature range over many orders of magnitude. Direct measurements of molecular weight have produced conflicting results due to the tendency of asphaltenes to form aggregates. This ambiguity has led to the emergence of at least three well established models which are mutually exclusive yet consistent with the spectroscopic data. The first of these models may be described as the ‘giant molecule’ picture.⁵ This model proposes that asphaltene molecules are composed of very large aromatic domains surrounded by very long aliphatic chains. The second model may be described as the ‘archipelago’ picture.⁶ This model proposes that asphaltene molecules are composed of many smaller aromatic cores which are covalently linked together by aliphatic chains. The final model may be described as the ‘small molecule’ or monomer description.^{7–9} In this case, asphaltene molecules are assumed to have a single aromatic core with short aliphatic side chains.

Historically, the first two models have had wide acceptance as they are consistent with vapor pressure osmometry (VPO) measurements and other common methods used to measure molar concentration. However, rotational diffusion constants of asphaltene molecules measured by fluorescence depolarization have been found to be small⁷ and suggest small molecules; a recent NMR study⁸ supports this picture. These rotational diffusion measurements are incompatible with large, rigid molecules implied by the ‘giant molecule’ paradigm. Nevertheless, it has been proposed that the ‘archipelago’ model—with islands of fused aromatic ring systems connected by loose alkane linkages—might be compatible with large molecules characterized by subunits with small rotational diffusion constants.⁶

More recent experiments based on ultrasonic sound velocity measurements, AC conductivity, and NMR all suggest that there is a physical transition at approximately 0.15–0.20 g/L.^{10,11,8} This so-called critical nanoaggregate concentration (CNAC) makes VPO measurements less reliable as typical concentrations required for these measurements exceed this by a factor of 100. Mass spectroscopy results—perhaps the most obvious candidate to determine asphaltene molecular weight—have been questioned based on two issues: the ability to obtain a gas phase of large components and possible fragmentation. Recent ultrahigh resolution mass spectroscopy results¹² found that the most abundant species of polar asphaltenes molecules are in the range 400–800 amu, supporting the rotational diffusion data.

To resolve these issues one must employ a technique which is nondestructive and remains sensitive at concentrations many orders of magnitude below the presumed CNAC and below the presumed onset of dimer formation (0.05 mg/L¹³). To this effect, we study the translational diffusion of asphaltene molecules using fluorescence correlation spectroscopy (FCS) at extremely low concentrations (as low as 0.03 mg/L) in toluene. This technique uses fluorescence to measure molecular diffusivities; one can thus infer a molecular ‘size’ without ambiguities arising from aggregation or fragmentation.

Experimental Background

FCS analyzes the time-dependent fluctuations in the fluorescence intensity collected from a sample driven either by Brownian motion or chemical kinetics. For noninteracting

* Corresponding author e-mail: bandrews@slb.com.

[†] Schlumberger-Doll Research.

[‡] Harvard University.

particles at a given average concentration C , the relaxation of local fluctuations in the concentration around the ensemble average $\delta C(r, t)$ is governed by the diffusion equation:

$$\frac{\partial \delta C(r, t)}{\partial t} = D \nabla^2 \delta C(r, t) \quad (1)$$

Here D is the translational diffusion coefficient. The normalized autocorrelation function $G(\tau)$ is defined as a time average of the products of the fluorescence intensity $F(t)$ at different lag times τ .¹⁴

$$G(\tau) = \frac{\langle F(t)F(t+\tau) \rangle}{\langle F(t) \rangle^2} - 1 \quad (2)$$

Current FCS experiments utilize a confocal illumination and detection setup which restricts the collection of light to a small observation volume. Typically, one assumes this confocal observation volume to be a Gaussian ellipsoid:

$$I(r) = I_0 \exp\left(-\frac{2(x^2+y^2)}{w_{xy}^2} - 2\frac{z^2}{w_z^2}\right) \quad (3)$$

By combining the solution of eq 1 with eq 3, eq 2 can now be evaluated¹⁵

$$G(\tau) = \frac{1}{N} \left(1 + \frac{\tau}{\tau_D}\right)^{-1} \left(1 + \omega^2 \frac{\tau}{\tau_D}\right)^{-1/2} \quad (4)$$

where $N = VC$ is the mean number of the number of fluorescent molecules, $\omega = w_{xy}/w_z$ is the ratio of the beam waist in the transverse and axial directions, and $\tau_D = w_{xy}^2/4D$ is the characteristic time required for a molecule to cross the focal volume. This volume $V = \pi^{3/2} w_{xy}^2 w_z$ is typically on the order of 1 fL. The correlation function (eq 4) can be modified to take into account chemical kinetics, triplet formation, photobleaching, and polydispersity.^{16,17} τ_D is obtained by fitting the measured $G(\tau)$ to the functional form of eq 4 using least squares.

From τ_D , the diffusion constant is obtained by the relation

$$D = \frac{w_{xy}^2}{4\tau_D} \quad (5)$$

If the molecule is approximated as a sphere, a hydrodynamic radius may be inferred from the diffusion constant D using the Stokes–Einstein equation¹⁸

$$R = \frac{k_B T}{6\pi\eta_s D} \quad (6)$$

where D is the diffusion constant, k_B is the Boltzmann constant, T is the temperature, η_s is the solvent viscosity, and R is the radius of the sphere.

In practice, neither the focal nor the observation volumes are perfectly Gaussian, so the measured autocorrelation functions will contain artifacts which are not taken into account by eq 4. Analysis of the effects of focal volume artifacts on the correlation function have been explored in detail by Koppel¹⁹ and Hess et al.²⁰ (and references therein). These artifacts make precise determination of all fit parameters challenging. Moreover, the large number of fit parameters typically utilized makes precise and unambiguous determination of a diffusion constant nearly impossible. Below, we use a scaling technique to overcome this limitation.

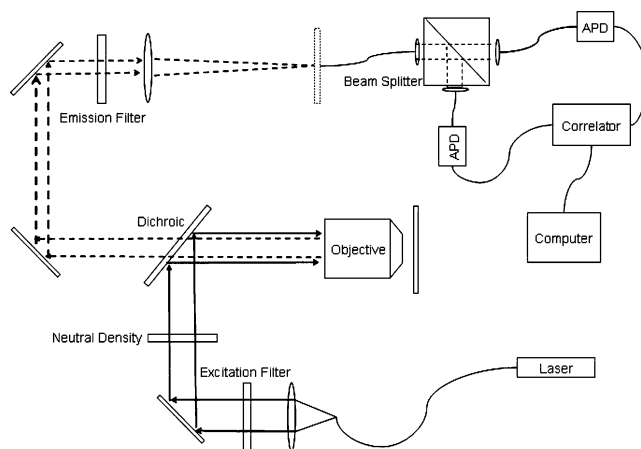


Figure 1. Schematic of experimental apparatus. The 405 nm diode laser is collimated to slightly underfill the back aperture of the 60× objective. Cross-correlation is obtained with a beam splitter and two APDs.

Our FCS measurements are performed on a home-built apparatus similar to those described elsewhere (Figure 1).²¹ A 405 nm, 20 mW diode laser (New Focus) is coupled to the optical assembly via single mode fiber (OZ Optics) and collimated to a diameter which slightly underfilled the back aperture of the objective (60 × 1.42NA oil Plan Apo from Olympus). The dichroic, excitation, and emission filters were obtained as a matched set from Chroma Technology corporation. Instead of a pinhole, a multimode fiber is coupled to a beam splitter and dual avalanche photodiodes (Pacer) with the outputs cross correlated. Fluorescent polyspheres with sizes ranging between 0.025 and 0.3 μm (Duke Scientific) and carboxytetramethyl-rhodamine dye (Fluka) were used for preliminary characterization during instrument construction.

Our sample dilutions are prepared in HPLC grade toluene purchased from Aldrich and used as is. Asphaltene concentrations range between 0.03 and 3.0 mg/L. For reference we measure dyes with absorption band maxima near our laser excitation wavelength (405 nm). We select chromophores with a wide range of molecular diffusivities in order to juxtapose the diffusion curves of these heavier and lighter compounds with the asphaltenes. The chromophores include perylene and octaethyl-porphyrin (OEPorphyrin) (Sigma-Aldrich). Quantum dots from Evident Technologies (620 nm emission core–shell CdSe/ZnS) are also utilized. The asphaltene samples are prepared by precipitation from crude oil with *n*-heptane. Specifically, UG8 (Kuwait) asphaltene is examined. Asphaltene samples are naturally fluorescent and do not require tagging with tracer molecules.

The optical properties of crude oils and asphaltenes have been reviewed extensively by Mullins et al. (ref 2 and references therein). The choice of 405 nm wavelength for our FCS experiments is dictated by two considerations: (1) Absorption spectra of asphaltenes drops exponentially at longer wavelengths starting at 650 nm, thus near-infrared wavelengths are of less interest.²² (2) Due to the lack of small ring systems,²³ fluorescence emission spectra of asphaltenes have almost no UV component. Previous work has shown that excitation at 400 nm and detection of all optical wavelengths above 450 nm comprises almost all of the asphaltene fluorophores. Blue emitting chromophores in asphaltenes have larger quantum yield (by the energy gap law) so our choice of a long pass emission filter emphasizes the smaller ring systems.

Scaling Analysis

As noted above, it is standard practice to fit the observed correlation function $G(\tau)$ to a Gaussian-Gaussian correlation function (GGCF) as described by eq 4. This function is derived assuming that the observation volume is a three-dimensional Gaussian ellipsoid. However, it has been pointed out that this approximation is often not valid and leads to discrepancies between the observed data and fits to the GGCF.^{20,24,25} This is aggravated by optical aberrations, most commonly due to refractive index mismatch²⁶ and imperfect alignment. For example, index mismatch leads to substantial increase in the contribution from the out of focus region. These systematic deviations from the GGCF can lead to artifacts and misleading conclusions such as anomalous diffusion. We therefore reanalyze the data using a scaling assumption (see below) that is independent of eq 4 and thus less sensitive to optical artifacts. This method is applicable when only a single diffusing species is present and there are no chemical reactions.

We present a brief but rigorous argument concerning the scaling behavior of the two time correlation function obtained by FCS for free (bulk unrestricted, nonreacting) diffusion; this argument does not require detailed treatment of the optical system and determines the diffusion coefficient of the unknown molecule by scaling the data with respect to that of a known standard. The details of the argument will be published elsewhere.²⁷

The observed $G(\tau)$ is given by the convolution²⁰ of $\mathcal{A}(\vec{r}_1, \vec{r}_2, \tau)$ —the two point correlation function or the propagator of density fluctuations—with $\mathcal{O}(\vec{r}_1, \lambda_{\text{em}}, \lambda_{\text{ex}})$ $\mathcal{O}(\vec{r}_2, \lambda_{\text{em}}, \lambda_{\text{ex}})$ where $\mathcal{O}(\vec{r}, \lambda_{\text{em}}, \lambda_{\text{ex}})$ is the observation volume or optical response function for a point \vec{r} , excitation wavelength λ_{ex} , and an emission wavelength λ_{em} . In the present case, it suffices to note that for free diffusion, τ appears in $\mathcal{A}(\vec{r}_1, \vec{r}_2, \tau)$ only as a product $D\tau$ i.e., multiplied by the diffusion coefficient D . Furthermore, $\mathcal{A}(\vec{r}_1, \vec{r}_2, \tau)$ is proportional to the concentration of chromophores. If we assume that the emission and excitation wavelengths are constant or nearly constant $G_a(\tau) = G(D_a\tau)$ and $G_b(\tau) = G(D_b\tau)$ of two different molecules will fall on each other when $\ln(D_a\tau)$ and $\ln(D_b\tau)$ are shifted in proportion to their diffusion coefficients and concentrations. Thus, if the diffusivity of at least one of the molecules is known, then that of the others is determined by the magnitude of the shift. For a single diffusing species this procedure makes it possible to compare diffusivities without fitting the data.

Results and Discussion

Figure 3 compares the diffusion curves for asphaltenes with known fluorophores with their concentrations equalized. The first thing to note is that the diffusivity of UG8 asphaltene is comparable to OEPorphyrin ($R_h = 7.5$ Å). The diffusion constant for perylene ($R_h = 3.5$ Å) is smaller than UG8 asphaltene, while that of quantum dots ($R_h = 50$ Å) is much larger. Thus FCS easily measures the range of molecular sizes which straddle the asphaltenes. The similar diffusivities of asphaltene and OEPorphyrin alone suggest that their hydrodynamic sizes are similar. Considering that porphyrins and asphaltenes have similar densities, this suggests that asphaltene molecules probed by this technique have molecular weights of the same order of magnitude as that of OEPorphyrin. Most importantly, aggregation effects can be neglected, as there is no concentration dependence in the diffusion times measured by FCS for concentrations spanning the range of 0.03–3.0 mg/L.

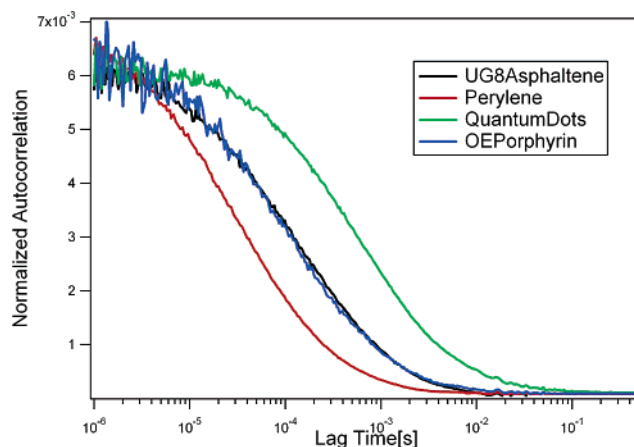


Figure 2. Diffusion curves for perylene (red), OEPorphyrin (blue), UG8 asphaltene (black), and quantum dots (green). The amplitudes have been “normalized” by adjusting the y values so that normalized autocorrelation appears the same for each sample. This is the first step in the scaling analysis described in the text.

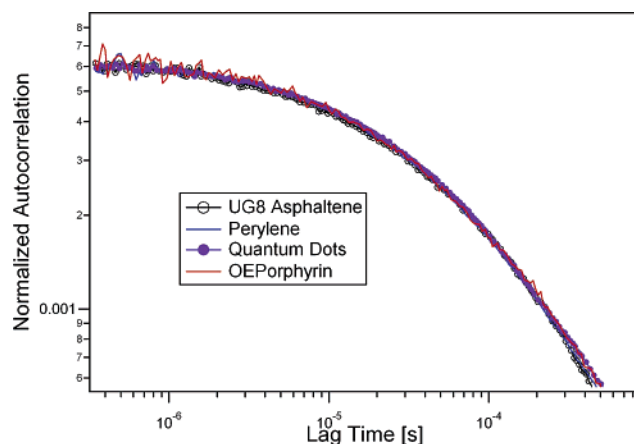


Figure 3. The four diffusion curves shown in Figure 2 scaled onto perylene as described in the text (log–log plot): perylene (red), OEPorphyrin (blue), UG8 asphaltene (black), and quantum dots (green).

Figure 3 shows the same data appearing in Figure 2 after scaling diffusion times as discussed above. We do not show the data when the normalized correlation falls below 10^{-4} because at such low concentrations, the data are noisy. Figure 4 shows fits to our data with eq 4, using the traditional method of least squares. Several combinations of parameters can produce equally plausible fits. Table 1 summarizes the relative diffusivities obtained from least squares (column 3) and using the scaling method described above (column 4). The two methods yield nearly identical diffusivities; however, the scaling procedure has the advantage that the results do not depend on the choice of a model function and are parameter independent.

Using eq 6, the hydrodynamic diameter can be estimated to be 21 Å. This is comparable to the diameter inferred from rotational diffusion constants using fluorescence depolarization (FDP) by Groenzin,⁷ 16(18) Å for spherical (ellipsoidal) geometry. The 15% difference in hydrodynamic radii obtained by FCS and FDP can be attributed to the different sensitivities that rotational and translational diffusion have to the asymmetry of the asphaltene molecule and is well within the errors inherent to the assumption of spheroidal particles. Moreover, the FDP studies⁷ used a band-pass emission filter which omits the contribution of larger chromophores at this wavelength. Nonetheless, both FCS and FDP conclude that the asphaltene fluorophores have hydrodynamic radii close to typical porphyrin

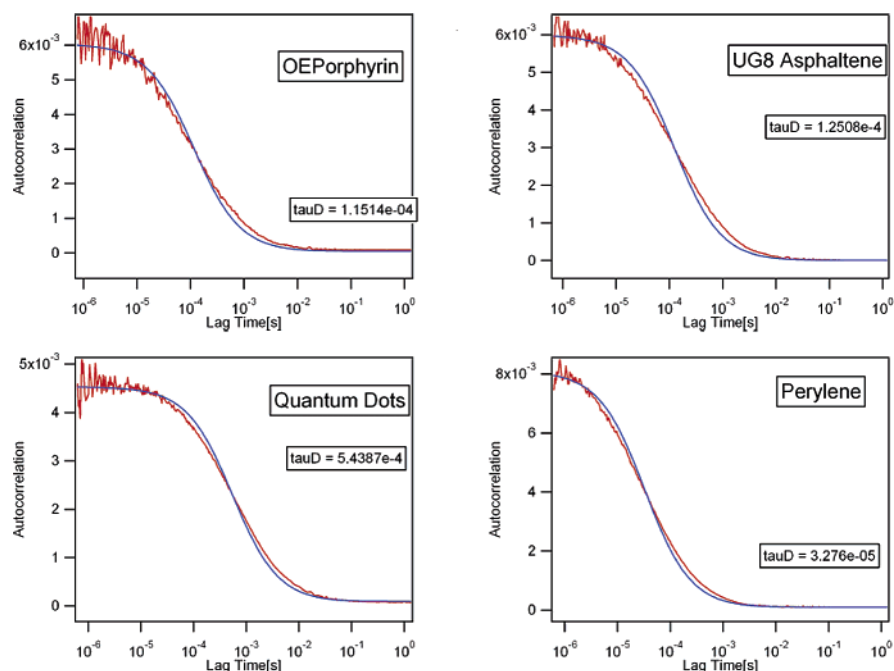


Figure 4. Unscaled diffusion curves for (a) OEPorphyrin, (b) UG8 asphaltene, (c) quantum dots, and (d) perylene showing the results of a traditional least-squares fits to eq 4.

TABLE 1: Diffusion Times (Column 2) and Diffusion Constants (Column 3) Obtained by Fitting the Data in Figure 4 Using Least Squares^a

	τ_D (10^{-5} s)	D (10^{-5} cm ² /s)	D (10^{-5} cm ² /s)
perylene	3.27	1 (1.29)	1 (1.29)
OEPorphyrin	11.5	0.28 (0.37)	0.29 (0.37)
asphaltene	12.5	0.26 (0.34)	0.27 (0.35)
quantum dots	54.4	0.06 (0.08)	0.06 (0.08)

^a Relative diffusivities are derived from the diffusion times listed in column 2. Column 4 gives the diffusion constants derived from the scaling procedure described in the text. Parentheses give the diffusivities scaled with respect to published values for perylene.²⁸

TABLE 2: Comparison of Diffusion Times Obtained for Asphaltenes from Three Different Techniques^a

method	D (10^{-5} cm ² /s)	concn (g/L)	d (Å)
FDP ⁷		0.006	16–18
FCS	0.35	0.00003	21
NMR ⁸	0.29	0.05	24

^a FCS and FDP measurements were performed at identical excitation wavelength; however, in the latter case a bandpass emission filter was used. All samples were prepared from the same crude oil – UG8.

molecules. While in the archipelago model individual aromatic rings may contribute small rotational diffusivities, and translational diffusion must scale with the size of the archipelago. Consequently, measurement of translational diffusion (FCS) resolves ambiguities present in the rotational diffusion measurements (FDP). Having nearly identical rotational and translational hydrodynamic radii is only consistent with the ‘small molecule’ picture, since the entire molecule is probed for the latter measurement.

Dimerization has been shown to occur at concentrations of 0.05 g/L¹³ using absorption and fluorescence spectroscopy. NMR data shows a mean dispersion constant $D = 0.29 \times 10^{-5}$ cm²/s.⁸ However, we do not observe any concentration dependence in the decorrelation times for the range of concentrations that our FCS apparatus is sensitive to: 0.03–3 mg/L. At higher concentrations the amplitude of the correlation function decreases below our noise floor, so we are unable to observe

dimerization. Table 2 compares the diffusion constants obtained from FCS with fluorescence depolarization (FDP)⁷ and nuclear magnetic resonance (NMR).⁸

Conclusions

The translational diffusion constants for asphaltenes are small and comparable to previously measured rotational diffusion constants. This suggests that there is no internal structure of chromophoric groups in asphaltenes beyond single aromatic cores. This result is incompatible with the archipelago type structures proposed in the literature. Similarly, very large ring systems with correspondingly high molecular weights—which would exhibit slower diffusion constants for both rotational and translational diffusion—are likewise inconsistent with our data. Together, the rotational and translational diffusion constant measurements show that these molecules are monomeric, not polymeric.

The concentrations employed here are as low as 100 times below the concentrations suggested for dimer formation and are the lowest reported in the literature to date. This ensures that our data are free of the complications caused by molecular aggregation and interfacial phenomena. At the concentrations accessible to traditional techniques aggregates are often mixed in with single molecules, which impedes the determination of monomeric sizes. We believe that self-assembly of asphaltene molecules is responsible for the wide range of molecular sizes and weights reported in the literature.

Acknowledgment. We thank Professor D. Weitz for help with building the FCS and Dr. B. Dasgupta for help in the early stages of building the apparatus. We also thank Y.-Q. Song, D. Freed, and N. V. Lisitza for useful discussions.

References and Notes

- (1) Sheu, E. Y. *Phys. Rev. A* **1992**, 45, 2428.
- (2) Mullins, O. C.; Sheu, E. Y. *Structure and Dynamics of Asphaltenes*; Springer: New York, 1998.
- (3) Rogel, E. *Langmuir* **2004**, 20, 1003.

- (4) Mullins, O. C.; Sheu, E. Y.; Hammami, A.; Marshall, A. G. *Asphaltenes, Heavy Oils and Petroleomics*; Springer: New York, 2006; in press.
- (5) Morgan, T. J.; Millan, M.; Behrouzi, M.; Herod, A. A.; Kandiyotti, R. *Energy Fuels* **2005**, *19*, 164.
- (6) Strausz, O. P.; Mojelsky, T. W.; Lown, E. M. *Fuel* **1992**, *71* (12), 1355.
- (7) Groenzin, H.; Mullins, O. C. *J. Phys. Chem.* **1999**, *103*, 11237.
- (8) Lisitz, N. V.; Freed, D. E.; Sen, P. N.; Song, Y.-Q. *Self-assembly of Asphaltene: Enthalpy, Entropy of Depletion and Dynamics at Crossover*. **2006**, to be submitted.
- (9) Qian, K. R.; Rogers, P.; Hendrickson, C. L.; Emmett, M. R.; Marchall, A. G. *Energy Fuels* **2001**, *15*, 492.
- (10) Andreatta, G.; Bostrom, N.; Mullins, O. C. *Langmuir* **2005**, *21* (7), 272.
- (11) Sheu, E.; Long, Y.; Hamza, H. *Asphaltene Self Association and Precipitation in Solvents - AC Conductivity Measurements*; 2006; see Chapter 10 in ref 4.
- (12) Rogers, R. P.; Marshall, A. G. *Petroleomics: Advanced Characterization of Petroleum Derived Materials by Fourier Transform Ion Cyclotron Resonance Mass Spectrometry*; 2006; see Chapter 3 in ref 4.
- (13) Goncalves, S.; Castillo, J.; Fernandez, A.; Hung, J. *Fuel* **2004**, *83*, 1823.
- (14) Elson, E. L.; Magde, D. *Biopolymers* **1974**, *13*, 1.
- (15) Eigen, M.; Rigler, R. *Proc. Natl. Acad. Sci.* **1994**, *91*, 5740.
- (16) Schwille, P.; Haustein, E. *Fluoresc. Correlation Spectrosc.* **2000**, *1*, 1.
- (17) Krichesky, O.; Bonnet, G. *Rep. Prog. Phys.* **2002**, *65*, 251.
- (18) Einstein, A. *Ann. Phys.* **1905**, *17*, 549.
- (19) Koppel, D. E. *Phys. Rev. A* **1974**, *10*, 1938.
- (20) Hess, S. T.; Webb, W. W. *Biophys. J.* **2002**, *83*, 2300.
- (21) Sengupta, P.; Ballaji, J.; Maiti, S. *Methods* **2002**, *27*, 374.
- (22) Mullins, O. C.; Mitra-Kirtley, S.; Zhu, Y. *Appl. Spectrosc.* **1992**, *46*, 1405.
- (23) Ralston, C. Y.; Wu, X.; Mullins, O. C. *Appl. Spectrosc.* **1996**, *10*, 1563.
- (24) Hong, H.; Elson, E. L. *Appl. Opt.* **1991**, *30* (10), 1191.
- (25) Perroud, T. D.; Huang, B.; Wallace, M. I.; Zare, R. N. *ChemPhys-Chem* **2003**, *4*, 1121.
- (26) Wiersma, S. H.; Visser, T. D. *J. Opt. Am. A* **1996**, *13* (2), 320.
- (27) Guerra, R. E.; Sen, P. N.; Andrews, A. B. Manuscript in preparation.
- (28) Hejtmanek, V.; Schneider, P. *J. Chem. Eng. Data* **1993**, *38*, 407.